Separation and Purification Technology 235 (2020) 116203

Contents lists available at ScienceDirect

Separation and Purification Technology

journal homepage: www.elsevier.com/locate/seppur

Cryogels with high cisplatin adsorption capacity: Towards removal of cytotoxic drugs from wastewater

Tania Farías[a,b], Solmaz Hajizadeh[a,*], Lei Ye[a]

[a] Division of Pure and Applied Biochemistry, Department of Chemistry, Lund University, Sweden
[b] Institute of Materials Science and Technology, University of Havana, Havana, Cuba

ARTICLE INFO

Keywords:
Cryogel
Cisplatin
Wastewater treatment
Pharmaceutical

ABSTRACT

Macroporous cryogels for capturing cisplatin were synthesized by cryogelation polymerization of methacrylic acid and 2-hydroxyethyl metacrylate. The cryogel materials exhibited good mechanical property, high swelling ratio and high affinity for cisplatin, with an adsorption capacity of up to 150 mg cisplatin per gram of cryogel. The correlation between the capacity of the cryogel and the monomer composition in the material was investigated in this study. The physical and chemical properties of the cryogels were studied in detail using scanning electron microscopy, textural analysis and infrared spectroscopy. The optimal cryogel can be reused for at least 14 cycles of adsorption/desorption to remove cisplatin from water without noticeable reduction of capacity. The experimental results suggest that the cryogel may be used as affinity adsorbents to remove cisplatin from wastewater discharged from pharmaceutical manufacturers and hospitals.

1. Introduction

Cisplatin (cis-diammine-dichloroplatinum(II)) belongs to the cytotoxic drug category and has been used for cancer treatment for over 30 years [1]. Multiple mechanisms have been suggested for the complex activities of this drug in the body. However, the critical mechanisms of cisplatin are DNA damage and the associated DNA damage response [2]. Although cisplatin is an effective cancer drug, it imposes a threat to the ecosystem and human health due to its capability of direct and uncontrolled damaging of DNA. In addition, the low biodegradability, high toxicity and low selectivity for therapeutic targets make cisplatin one of the most challenging drug contaminants in wastewater [3]. Today, cisplatin is considered as an emerging water contaminent and its presence has already been recorded in surface water, hospital sewage system and wastewater treatment plants in the range of ng/L to μg/L, respectively [4–7]. Therefore, it is crucial to find an effective and practical way to remove cisplatin from wastewater streams at the sources e.g. hospitals and manufacturing plants before the drug enters drinking water and food chain.

To tackle the problem of water contamination, different technologies based on (a) biological treatment, (b) physico-chemical separation, and (c) advanced oxidation processes have been proposed for removal of different cytotoxic drugs [8] such as membrane bioreactor (MBR) [9,10], adsorbents based on powder or granular activated carbon [11,12], membrane filtration [13,14], electrodialysis [15], ozonation [16], catalytic oxidation [17], etc. MBR and electrodialysis have been reported earlier for removing cisplatin from hospital wastewater effluent [10,18]. However, the efficiency of removal by MBR was reported to reach only around 51–63% of total platinum. Besides, the drug showed negative effects on the microbial community on the membrane [19]. Although electrolysis showed higher removal efficiency, its operational cost is considerably higher in comparison with the other techniques [18]. Therefore, there is still a need for alternative technology for removing cisplatin from the wastewater stream, which has high efficiency yet being simple and inexpensive.

As one special type of macroporous hydrogel, cryogel is composed of a polymer network with well-controlled macroporosity (with pore sizes between 1 and 100 μm). The large pores in cryogels are formed during cryogelation polymerization at sub-zero temperature. This macroporous structure is stable at room temperature, and due to the large porous structure, it enables efficient mass transfer [20]. In addition, the macrometers size of the interconnected channels allows the passage of particulate-containing fluids such as wastewater at a high flow rate with low back pressure [21–25]. These unique properties of cryogel make it possible to realize direct removal and separation of a target molecule from complex samples without any pre-treatment step. In this study, a cryogel composed of methacrylic acid and 2-hydroxyethyl metacrylate was prepared for removing cisplatin from water

* Corresponding author.
E-mail address: Solmaz.hajizadeh@tbiokem.lth.se (S. Hajizadeh).

https://doi.org/10.1016/j.seppur.2019.116203
Received 4 September 2019; Received in revised form 7 October 2019; Accepted 10 October 2019
Available online 10 October 2019

samples. The cryogel was designed based on the physico-chemical adsorption mechanism of cisplatin. The properties of the cryogel material were studied, as well as its binding capacity towards cisplatin and the regeneration of the cryogel after multiple rounds of adsorption/desorption processes.

2. Material and methods

2.1. Material

Methacrylic acid (MAAc, 98.5%), 2-hydroxyethyl methacrylate (HEMA, ≥99%), *N,N'*-methylenebisacrylamide (MBA, 99%), *N,N,N',N'*-tetramethyl ethylene diamine (TEMED, 99%), ammonium persulfate (APS, ≥98.0%), sodium chloride (NaCl, ≥99.0%), sodium acetate (NaAc, ≥99.0%) and acetic acid (HAc, ≥99.0%) were purchased from Sigma-Aldrich and were used without further purification. Cisplatin (raw material for the pharmaceutical industry produced in China) was provided by the Center for Pharmaceutical Research and Development of Cuba (CIDEM).

2.2. Synthesis of poly(HEMA-co-MAAc) cryogel

The cryogels were synthesized using methacrylic acid (MAAc) and 2-hydroxyethylmetacrylate (HEMA) and *N,N'*-methylenebisacrylamide (MBA) as crosslinker by free radical polymerization. *N,N,N',N'*-tetramethyl ethylene diamine (TEMED) and ammonium persulfate (APS) were utilized as an activator and initiator, respectively. Different monomer compositions were used to prepare the macroporous hydrogels (Tables 1 and S1), where the molar ratio between MAAc and HEMA was varied from 0:10, 3:7, 4:6 to 5:5, and the molar ratio between (MAAc + HEMA) and MBA was changed from 20:1 to 8:1, while the total monomer concentration was kept at 10% (wt/v). The concentrations of APS and TEMED were fixed at 2% (wt/wt) with respect to the total monomers.

The monomers and the crosslinker were dissolved in water. The pH of the mixture was adjusted to (6–7) by using 5 M sodium hydroxide (NaOH) solution before adding the initiator. Then the mixture was cooled in an ice bath while it was purged by a gentle stream of nitrogen gas for 20 min. The APS solution (500 μL) was added to the mixture at the final stage. Aliquots (0.5 mL) of the solution were transferred into pre-cooled glass tubes (i.d. 7 mm) and frozen at −15 °C in a cryostat overnight. Once the reaction was completed the tubes were defrosted at room temperature. The cryogels were washed with distilled water several times to remove the excess of un-reacted chemicals. All cryogels were dried in an oven at 50 °C until constant weight. The cryogels that only contain HEMA as the monomer was dried by freeze-drier.

2.3. Cryogel characterization

Polymerization yield for each cryogel was calculated based on the equation below:

$$Y(\%) = \frac{W_1}{W_0} \times 100 \tag{1}$$

where W_0 and W_1 are theoretical weight and the dry weight of the cryogels, respectively.

Scanning electron microscopy (SEM) was used to study the morphology of the macroporous gels. The wet samples were cut into thin discs (1–2 mm thick) and freeze-dried. The dried samples were sputtered with gold: platinum (40:60, 15 nm thickness) and inspected using a JEOL JSM-80 5600 LV microscope (Tokyo, Japan).

Attenuated total reflection (ATR) infrared spectra were recorded at room temperature on a Thermo Fisher-Scientific FT-IR instrument (Thermo Fisher-Scientific Inc., Waltham, USA). All spectra were collected in the 4000–500 cm^{-1} wavenumber region with a resolution of 4 cm^{-1} and with 16 scans.

To determine the swelling degree of the cryogels, dried cryogel was weighed and immersed in distilled water and left for one hour at room temperature to ensure complete swelling. Then it was removed from the water and the excess surface water was removed by soaking with filter paper before the swollen cryogel was weighted again. Three replications were made in each case. The swelling degree was calculated using Eq. (2):

$$S_w = \frac{W_2 - W_1}{W_1} \tag{2}$$

where W_1 and W_2 are the weight of the dried and swollen cryogel, respectively.

To study the mechanical stability of the gels, a texture analyzer (XT2i, Stable Micro Systems, Godalming, England) was employed and Exponent, v.5.0.9.0 software (Godalming, England) was used for the data analysis. The cryogels were placed horizontally on a metal plate and a 2 kg load cell was applied at a speed of 1 mm/s at room temperature. The samples were compressed up to 70% of their original height. Texture analyzing test was done in duplicate. The Young's elasticity modulus was calculated in the linear range (Eq. (3)):

$$E = \frac{\sigma}{\varepsilon} = \frac{F/A_0}{\Delta l/l_0} \tag{3}$$

where E is Young's elasticity modulus (Pa), F is the force applied to the object (N), A_0 is the cross-sectional area on which the force is applied, Δl is the change in length under the compression and l_0 is the original height of the object.

2.4. Batch adsorption experiments

For batch adsorption of cisplatin, a dried cryogel was weighted and placed in a glass flask and hydrated with 0.5 mL of distilled water. Then an appropriate volume of cisplatin solution was added to the flask (the solid content of the sample was kept at 10 mg/mL). The flask was put on a rocking table at room temperature for 24 h. The solution after adsorption was measured by NanoPhotometer Pearl UV–Vis spectrophotometer (Germany) at 300 nm wavelength to determine the remaining concentration of cisplatin in the solution. The amount of the adsorbed drug on the gel was calculated by depletion method using Eq. (4):

$$\Gamma = \frac{(C_i - C_{eq})V}{m} \tag{4}$$

where Γ is the amount of cisplatin adsorbed (mg/g), C_i and C_{eq} are the cisplatin initial and equilibrium concentration (mg/mL), respectively, V is the volume of cisplatin solution (mL) put in contact with cryogel and m is the weight of the cryogel (g).

The initial concentrations of cisplatin for the batch adsorption were 0.25, 0.5, 0.75, 1, 1.5 and 2 mg/mL. Each solution was prepared by dilution of a 2 mg/mL cisplatin stock solution in distilled water. It should be noted that the stock solution was prepared 3 days in advance of the experiment in order to guarantee that the replacement of chloride ligands by water is complete and no changes in the UV spectrum was to take place. The cisplatin calibration curve was prepared from the same stock solution and measured at the same time as the samples.

Kinetic adsorption was studied on a selected cryogel with two different concentrations of cisplatin (0.5 and 2 mg/mL). The cryogel was left in contact with cisplatin solution for 1, 2, 4, 6, 8, 14, 20, 24, 30, 40 and 48 h before the unbound cisplatin in solution was measured as described above.

2.5. Desorption experiments

Desorption experiments were carried out in different media to find out the most effective solution to remove cisplatin from the cryogel. After cisplatin adsorption, each cryogel was rinsed with distilled water

(2 mL) to remove the cisplatin solution remained inside the cryogel's channels. Then the gel was put in a clean glass flask. Distilled water, 1 M NaCl, acetate buffer (0.1 M HAc, 0.005 M NaAc, pH 3.5) and 1 M NaCl in the same acetate buffer were selected as desorption solutions. The concentration and pH of the acetate buffer were kept constant throughout all the experiments. An appropriate volume of desorption solution (solid/liquid ratio at 10 mg/mL) was added to the cryogel, and the sample was left on a rocking table at room temperature for 24 h. The amount of desorbed cisplatin in the solution was measured with the spectrophotometer at 300 nm wavelength. The cisplatin calibration curve was prepared in respective to the medium in which the desorption experiment was carried out.

2.6. Repetitive adsorption-desorption experiments

For repetitive adsorption-desorption process, the selected cryogel was put in cisplatin solution (1 mg/mL) at a solid/liquid ratio of 10 mg/mL and kept for 4 h at room temperature on a rocking table. After this, the solution was collected and the concentration of cisplatin in solution was measured. The cryogel was rinsed first with distilled water (2 mL) and then treated with the desorption medium (2 mM NaOH or 1 M NaCl in acetate buffer) while keeping the solid/liquid ratio at 10 mg/mL. The experiment was carried out on the rocking table for 1 h at room temperature. The desorbed cisplatin was measured with the spectrophotometer. After the desorption step, the cryogel was rinsed with distilled water (2 mL) before starting a new adsorption-desorption cycle. The adsorption-desorption experiment was carried out in triplicate independent samples.

3. Results and discussion

3.1. Synthesis and characterization of cryogels

The large and interconnected channels of the cryogels provide a unique matrix for separation purposes when dealing with particulate-containing fluids such as wastewater. In comparison with conventional methods and materials such as filters and membranes, cryogels allow the sample mixture to pass through the polymeric matrices with a low back pressure without facing any fouling problem. Therefore, macroporous cryogels were selected as a potential material for removal of cisplatin from wastewater streams. The water-soluble monomers were selected based on their physico-chemical properties and possible molecular interactions with cisplatin, and their impacts on the architecture and stability of the resulting cryogel.

The poly(MAAc-co-HEMA) cryogel shows good stability and mechanical strength at room temperature. Based on visual inspection, the cryogels retained their physical forms after being dried, and do not disintegrate during the swelling process. Almost all the cryogels have a spongy texture except for the cryogel synthesized using only HEMA monomer, which appeared gelatinous. Digital image of the dried and fully swollen cryogel is presented in Fig. S1.

The yield of the cryogelation polymerization using different monomer compositions is presented in Table 1. High polymerization yield was obtained when the molar ratio of MAAc:HEMA was less than 5:5. No cryogel can be synthesized when the molar ratio of MAAc:HEMA is higher than 7:3. At high concentration, MAAc monomer is known to form dimers through hydrogen bonds [26]. This is probably the reason that caused the low yield of cryogel production. For the effect of the crosslinker, a slightly higher yield was reached when the amount of crosslinker was increased. This may be explained by the higher probability of the monomers to be incorporated into a living polymer chain [27].

The swelling degree and Young's elasticity modulus for the cryogels are presented in Table 1. In general, the swelling degree increases gradually with the MAAc content in the cryogel, which is coherent with the introduction of the ionizable carboxylic group in the cryogel. The electrostatic repulsion between $-COO^-$ groups at pH above its pK_a value (4.65) [28] increases the uptake of solvent into the polymer network [29]. However, for the cryogels with MAAc: HEMA molar ratio of 5:5 (cryogels C3 and C4), the swelling degree becomes lower, which may be due to the fact that at high MAAc concentration the carboxylic groups tend to interact via hydrogen bonds to form dimers [26]. The swelling degree decreases slightly when the concentration of the crosslinker increases. This is expected since there are more crosslinked bridges between the polymer chains, making the polymeric network to hold together more tightly [27]. Similar results have been reported by Yarimkaya and Basan for poly(2-hydroxyethyl methacrylate-co-acrylic acid-co-ammonium acrylate) hydrogels [30].

The elasticity modulus of the cryogels increases gradually when the concentration of MAAc increases. In addition, higher crosslinker concentration also resulted in higher elasticity modulus. Therefore, increasing the concentration of MAAc and the crosslinker strengthens the mechanical properties of the cryogels.

The SEM images of the cryogels show clearly the macroporous structure with evenly distributed pores separated by smooth and thin walls (Fig. 1). The heterogeneous pore size distribution of the cryogels was calculated between 10 and 100 μm based on the SEM images by using Image J software. The exact size distribution of the pores of a cryogel was analysed and reported elsewhere [31]. There were no significant differences in the porous structures when the concentration of the crosslinker was increased.

The IR spectra of the cryogels are presented in Fig. 2. The characteristic bands of the functional groups are present: νO—H (3400 cm^{-1}), νC—H (2984–2882 cm^{-1}), νC═O (1715 cm^{-1}), ν_{as} COO^- (1556 cm^{-1}), νCH_2 (1485 cm^{-1}), ν_s COO^- (1390 cm^{-1}), νC—O (1255 cm^{-1}), νC—O ester group (1160, 1076 cm^{-1}) and ρCH_2 (748 cm^{-1}). The presence of the band from ν_{as} COO^- indicates that the carboxylic group is deprotonated. The increase in the relative intensity of this band in sample C3 with respect to sample C7 is coherent with the increase of the molar ratio of MAAc from 30% to 50%. However, in the cryogel C1, the intensity of this band is lower, which may be related to the formation of hydrogen bonds between neighboring carboxylic groups when the amount of MAAc is increased. Note that the νC═O band for this sample has a shift towards higher wavenumbers, which supports the formation of hydrogen bonds.

3.2. Adsorption of cisplatin in the cryogels

Fig. 3A and B show the adsorption isotherms of cisplatin in the obtained cryogels. The concentration of cisplatin was measured by spectrophotometer at 300 nm wavelength (ε_{300} = 95.2 M^{-1} cm^{-1}). The shape of the isotherm curves with a steep slope denoted a great affinity of the adsorbents for cisplatin. The results show the importance of the presence of MAAc for cisplatin adsorption. Based on the adsorption isotherm of the HEMA-based cryogel, the capacity of the gel is very low for cisplatin adsorption. Introducing MAAc monomer to the HEMA cryogel increases the binding capacity noticeably. This result can be explained by the formation of a stable complex between cisplatin and the carboxyl group from MAAc, as has been reported previously [32–34]. As can be seen from the steepest binding isotherms, saturation binding cannot be measured due to the limited solubility of cisplatin in water [35]. Fig. 3B also shows that increasing the amount of crosslinker leads to a slight reduction of the cisplatin adsorption capacity (Fig. 3B). This result may be explained by the higher rigidity and firmness of the cryogel, which makes it more difficult for cisplatin molecules to diffuse inside the gels.

Fig. 4 shows the adsorption of cisplatin as a function of time on cryogel C3 for two different cisplatin concentrations. Cryogel C3 was selected for the kinetic studies considering it's physico-chemical properties and cisplatin binding capacity. The kinetic curves show a gradual initial increase in the amount of cisplatin adsorbed as a function of time, then a pseudo equilibrium is reached and later continue to

Table 1
Synthesis of cryogels and characterization of physical properties.

Cryogel	Molar ratio MAAc:HEMA	Molar ratio (MAAc + HEMA):MBA	Polimerization yield (%)	Sw (g/g)	E (kPa)
C1	7:3	20:1	36.0	N.A.	N.A.
C2		8:1	52.6	N.A.	N.A.
C3	5:5	20:1	95.2	24.6 ± 0.4	9.3 ± 1
C4		8:1	99.4	14.7 ± 1	15.6 ± 0.7
C5	4:6	20:1	81.0	26.2 ± 0.3	7.7 ± 0.5
C6		8:1	82.4	23.6 ± 0.5	9.7 ± 1
C7	3:7	20:1	93.7	21.4 ± 0.3	3.9 ± 0.1
C8		8:1	99.9	20.4 ± 0.3	10.5 ± 1
C9	0:10	20:1	95.6	12.1 ± 0.9	3.3 ± 0.2
C10		8:1	92.2	11.2 ± 0.3	5.2 ± 0.6

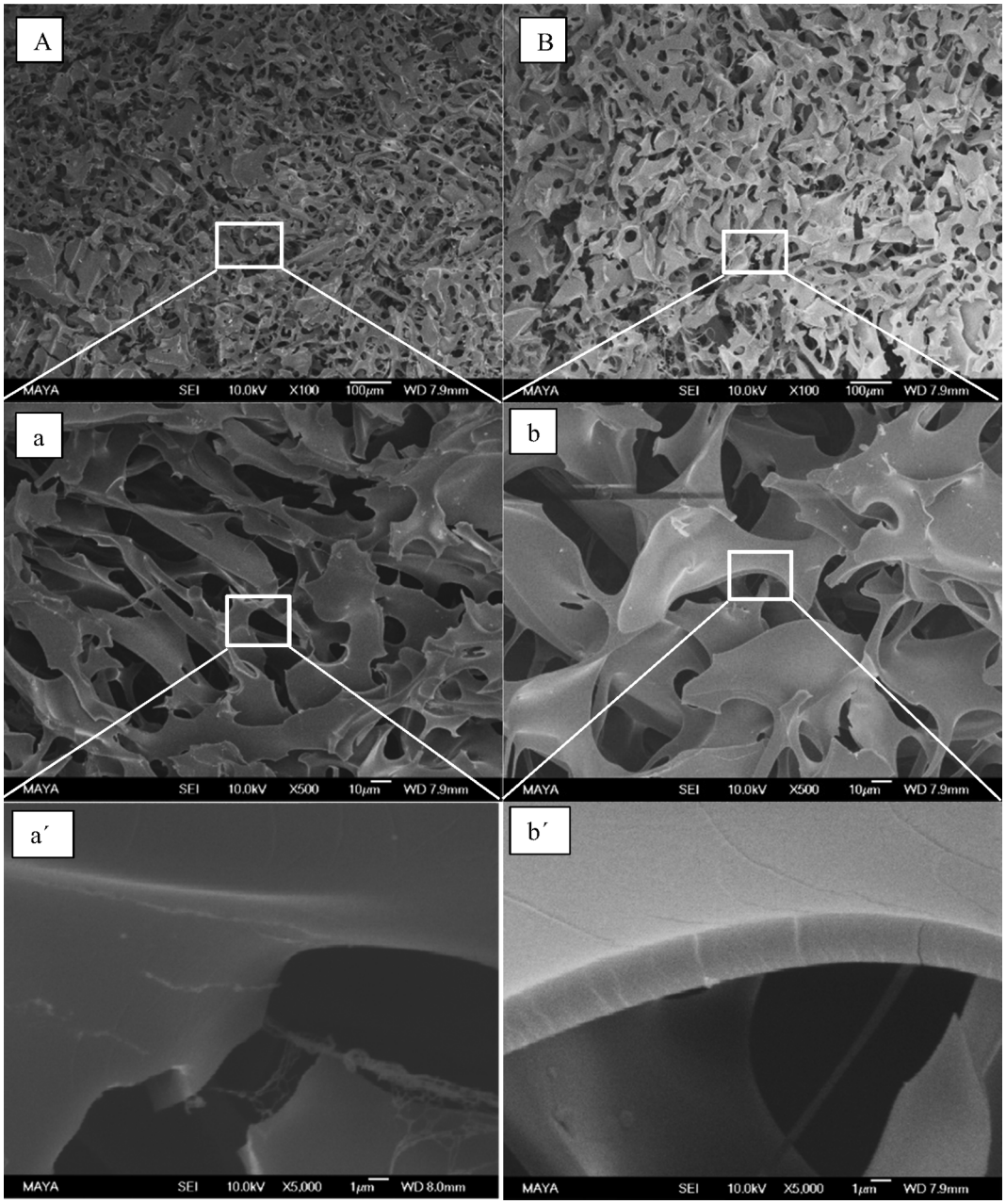

Fig. 1. SEM images of the cryogels at different magnifications. (A) Cryogel C3; (B) Cryogel C4. Images (a, a′) and (b, b′) are the image (A) and the image (B) at higher magnifications, respectively. The scale bars show 100, 10 and 1 μm, respectively.

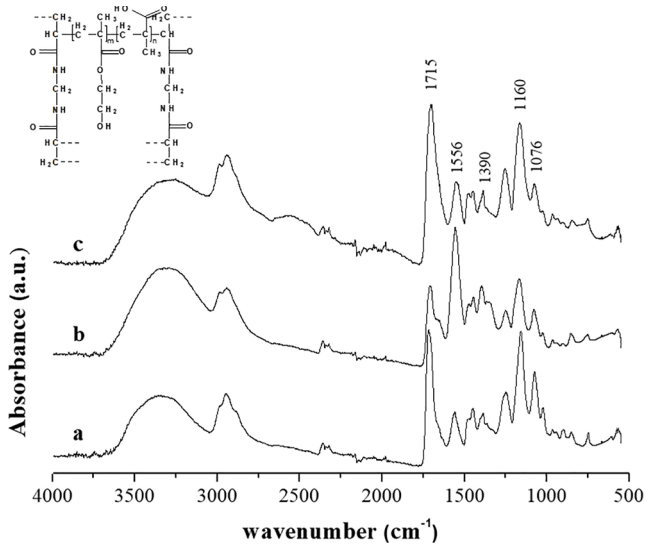

Fig. 2. ATR infrared spectra of cryogels: (a) cryogel C1, (b) cryogel C3 and (c) cryogel C7.

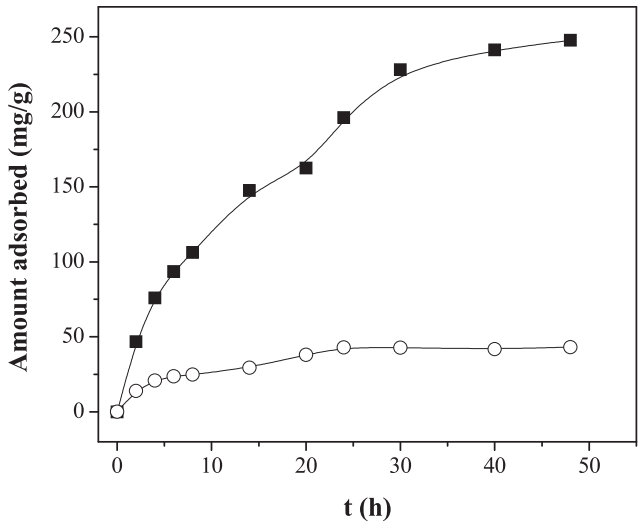

Fig. 4. The adsorbed amount of cisplatin as a function of time measured on cryogel C3 using two different initial cisplatin concentrations: -○- 0.5 mg/mL and -■- 2 mg/mL.

increase until reaching equilibrium at 24 and 48 h, for initial cisplatin concentrations of 0.5 and 2 mg/mL, respectively. The two-step saturation curve may be explained by the special cisplatin adsorption process. The first saturation occurs (ca 8 h and 20 h for initial concentrations at 0.5 and 2 mg/mL, respectively) on the surface of the cryogels where the mass transfer is high between the available carboxcylic groups on the surface of the cryogel and the free cisplatin. The second adsorption step is when the cisplatin molecules migrate from the surface to the interior of the hydrogel network through diffusion. The second step is slower and takes a longer time to reach equilibrium even though cisplatin is a small molecule (molecular weight 301 g/mol [36]).

To analyze the adsorption kinetic isotherm, different models were tested e.g. pseudo first order model [37], pseudo second order model [38], Elovich's equation [39] and intra-particle diffusion model [40]. The mathematical expressions of each model are summarized in Table S2, while the results of the fitting are presented in Fig. 5 and Table 2.

The pseudo first and pseudo second order kinetic models are the most widely used to describe the adsorption of a solute from a liquid solution [41]. In our case, comparison of the correlation coefficients obtained from the fitting with the two models for two different cisplatin concentrations (R^2 = 0.91 and 0.97 for pseudo first order, and R^2 = 0.94 and 0.98 for pseudo second order) indicates that the pseudo second order model describes the sorption data better. However, the sorption capacity predicted by this model is far from the experimental value for cisplatin concentration of 0.5 and 2 mg/mL (Table 2).

Elovich's equation based on chemisorption was established by Zeldowitsch [39] and has been used to describe the adsorption of gases on solid systems [42,43] and the adsorption process of pollutants from aqueous solutions [44,45]. This model was considered here due to the formation of complexes between cisplatin and the carboxyl groups of MAAc that was reported elsewhere [32–34]. The non-linear adjustment of our experimental data according to this model gave correlation coefficients greater than 0.90 for the two initial concentrations of cisplatin. If this equation is to become applicable, the data fitting should lead to a straight line for the amount adsorbed at time t (q_t) *vs.* ln *t*. However, in this study, different linear portions were obtained, which indicates that several steps may control the overall adsorption process. Therefore, it can be concluded that the chemisorption mechanism is not the limiting step of cisplatin adsorption.

The next model which was applied to fit the experimental data was the intra-particle diffusion model. In this model, plotting q_t *vs.* $t^{1/2}$ will give a straight line that passes through the origin if intra-particle diffusion is the sole rate-limiting step. When film diffusion takes place in this model, the intercept is θ, which is a constant related to the

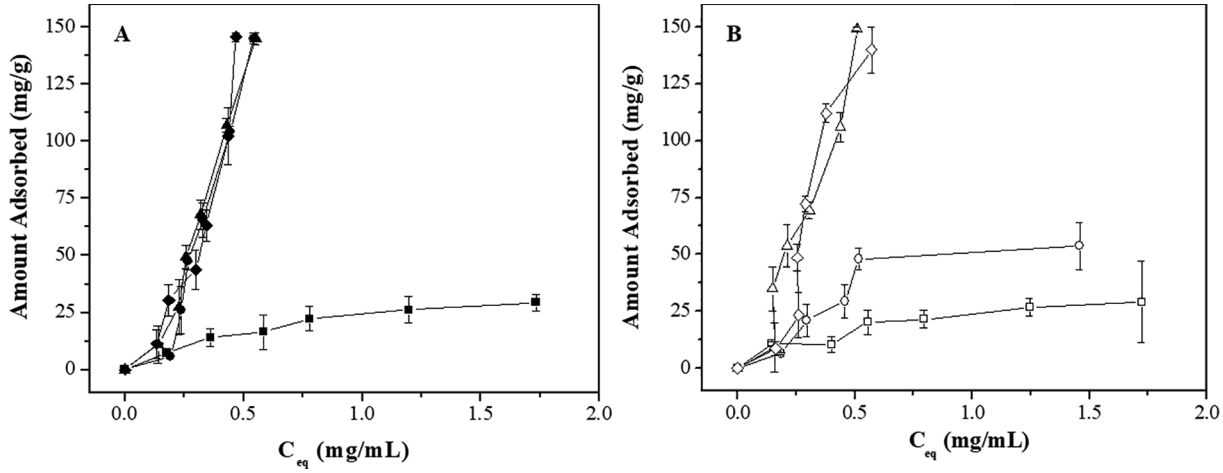

Fig. 3. Cisplatin adsorption isotherms of the cryogels prepared using different monomer compositions. The molar ratio of (MAAc + HEMA): MBA is (A) 20:1 (-◆- cryogel C3, -▲- cryogel C5, -●- cryogel C7 and -■- cryogel C9), and (B) 8:1 (-◇- cryogel C4, -△ - cryogel C6, -○- cryogel C8 and -□- cryogel C10).

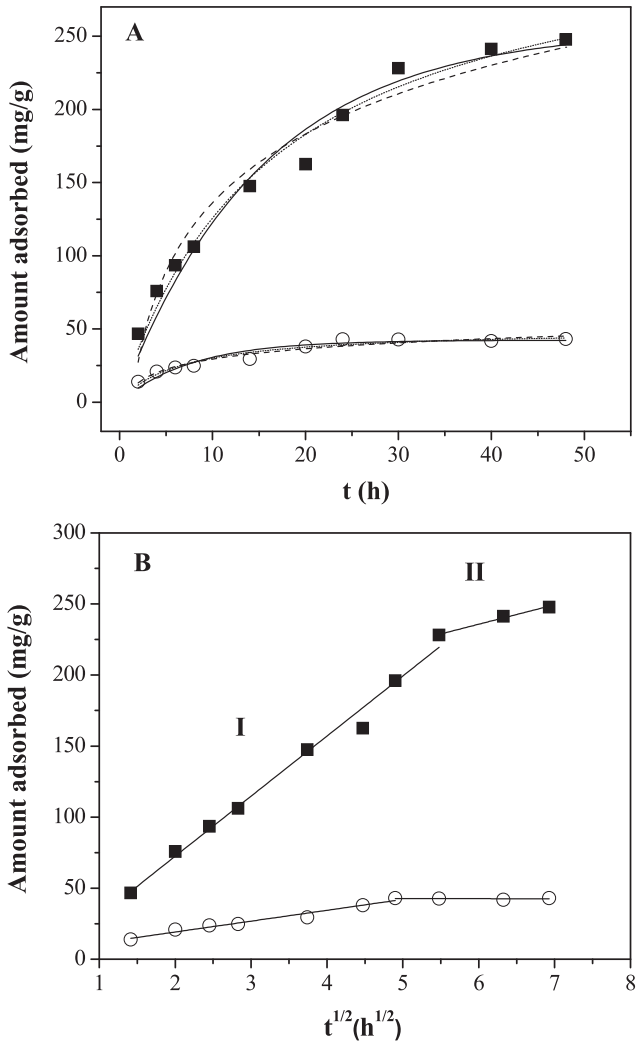

Fig. 5. Fitting of experimental data of cisplatin adsorption for two different initial concentrations of cisplatin: -○- 0.5 mg/mL and -■- 2 mg/mL. (A) Non-linear curve fit: — pseudo first order model, ····· pseudo second order model and —— Elovich's equation. (B) Fitting experimental data according to the intra-particle diffusion model (see Table S2), where I and II represent the two linear portions.

Table 2
Kinetic parameters obtained from data fitting for the adsorption of cisplatin on cryogel C3.

Kinetic models	Parameters	The initial concentration of Cisplatin	
		0.5 mg/mL	2 mg/mL
Pseudo first order	q_e (mg/g)	42 ± 2	255 ± 13
	K_1 (h^{-1})	0.13 ± 0.01	0.066 ± 0.001
	R^2	0.91	0.97
Pseudo second order	q_e (mg/g)	50 ± 2	334 ± 20
	K_2 (g/mg h)	0.003 ± 0.0005	0.0002 ± 0.00003
	R^2	0.94	0.98
Elovich's equation	α (mg/g h)	19 ± 3	51 ± 5
	$1/\beta$ (mg/g)	10 ± 1	67.7 ± 4
	R^2	0.94	0.96
Intra-particle diffusion	θ (mg/g)	43 ± 1	153 ± 4
	K_{id} (mg/g $h^{1/2}$)	0.1 ± 0.01	14 ± 1
	R^2	0.96	0.99

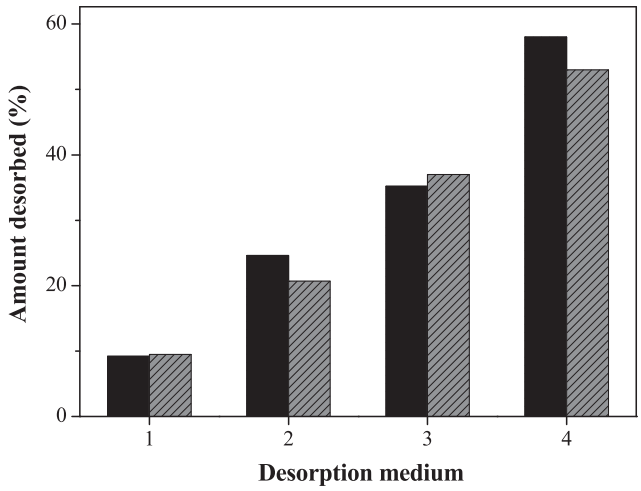

Fig. 6. Amount of cisplatin desorbed from two selected cryogels (gray: cryogel C3 and black: cryogel C7) in different desorption media: (1) distilled water, (2) 0.5 M NaCl, (3) acetate buffer and (4)1 M NaCl in acetate buffer. The amount of cisplatin available on the cryogels was calculated to be about 60 mg/g before the desorption experiment.

thickness of the boundary layer (see Table S2). In addition, if the data exhibit multi-linear plots, then two or more steps influence the sorption process. In our case, the plot of q_t *vs.* $t^{1/2}$ (Fig. 5B) shows two straight lines (I and II) and the plot does not pass through the origin. Therefore, we consider that the cisplatin adsorption occurs in two steps. The first step is related to gradual cisplatin adsorption where the intra-particle diffusion within the cryogel macro pores is rate-limiting, and the second step is where equilibrium is reached.

3.3. Desorption of cisplatin from the cryogels

The aim of this study is to use cryogels to remove cisplatin from water/wastewater streams. Reusing cryogels can be an interesting economical subject both from research and industry point of views. Therefore, the desorption of cisplatin from cryogel has to be considered. Fig. 6 shows the results of cisplatin desorption from cryogels C3 and C7 in different desorption media. The binding of cisplatin with the cryogel is very strong since the release is slow and difficult in distilled water. This confirms the formation of a complex between the drug and the carboxylic groups of methacrylic acid. In fact, desorption is slightly lower for the cryogel prepared using a MAAc:HEMA molar ratio of 5:5 (cryogel C3), which theoretically has a larger number of carboxylic groups available in the polymer matrix. In addition, the amount of cisplatin desorbed increases with the ionic strength of the desorption medium, due to the breakdown of the cisplatin:carboxylic acid complex.

3.4. Adsorption-desorption cycles

The adsorption-desorption studies were carried out in order to find out how many times the cryogel can be reused. Note that in the desorption step, the time for desorption was set at 1 h to be more realistic to real conditions. As presented earlier the maximum desorption can be reached to 60% after 24 h. The cryogel C3 was selected for this part of the experiment considering our previous results. Fig. 7 shows the adsorption-desorption graph of cisplatin for the selected cryogel, where 1 M NaCl in acetate buffer was used as the desorption medium.

In the first cycle, the cryogel adsorbs about 54 mg/g and around 30% of the loaded cisplatin is desorbed when the gel put in contact with the desorption medium for 1 h (Fig. 7). In the following cycles, the amount of cisplatin adsorbed is considerably reduced (to less than half of the amount adsorbed in the first cycle) while the percentage released

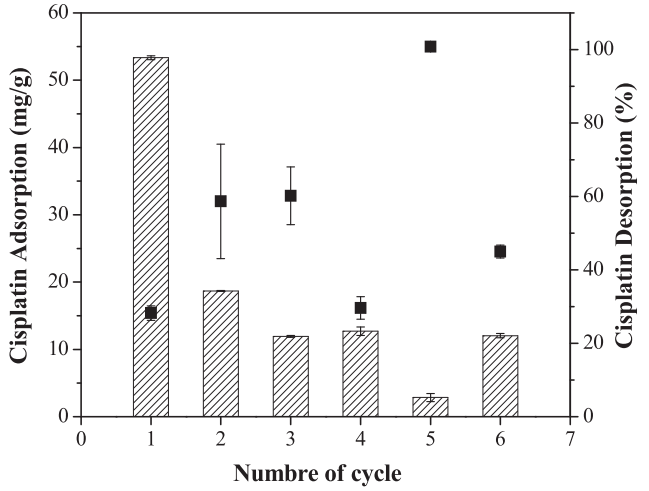

Fig. 7. Adsorption (bar graph)/desorption (scatter graph) of cisplatin on cryogel C3 using 1 M NaCl in acetate buffer as the desorption medium. For the adsorption step 1 mg/mL cisplatin solution was used.

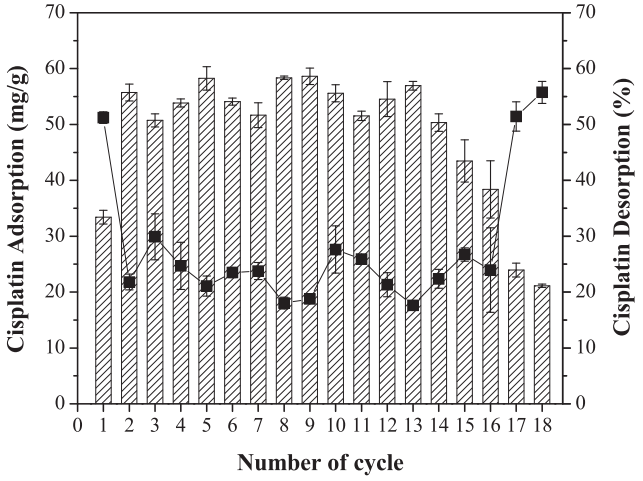

Fig. 8. Adsorption (bar graph)/desorption (scatter graph) of cisplatin in the cryogel C3 using 2 mM NaOH as the desorption medium. For the adsorption step, a 1 mg/mL cisplatin solution was used.

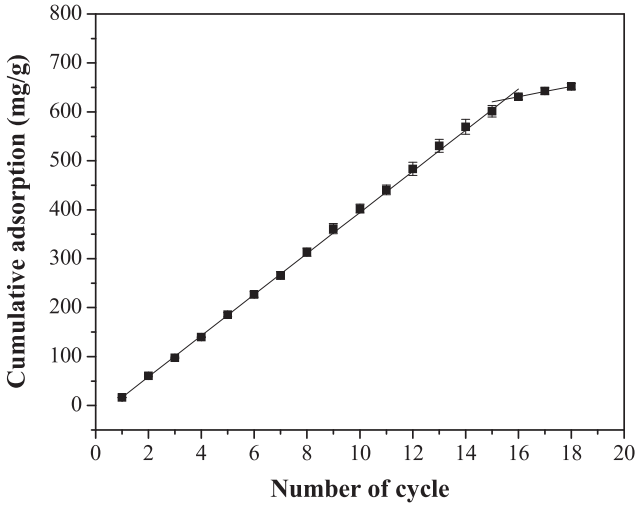

Fig. 9. Cumulative cisplatin adsorption by cryogel C3 during the adsorption-desorption study using 2 mM NaOH as the desorption medium.

increases. This behavior may be related to structural changes in the cryogel due to the treatment with the buffer solution. The pK_a of MAAc is about 4.65 [28], therefore at pH 3.5, the carboxylic groups in the cryogel are almost entirely protonated resulting in a neutral polymer, while at neutral or basic pH the carboxylic groups are deprotonated to make an anionic polymer. Taking into account that the most probable mechanisms of cisplatin adsorption in the cryogel is through the formation of a platinum complex with the carboxylic groups, it is then expected that the adsorption will be favored when the polymer is in its anionic form. On the other hand, it has been reported that the formation of two different types of carboxylic acid dimers within poly-methacrylic acid, which differ in their relative abundance, stabilities and acidities [26]. Based on ^{1}H solid-state NMR studies by Díez-Peña *et al.*, P-MAAc hydrogel changes from an expanded conformation at high pH to a compact contracted form at low pH, where hydrogen bonds play a central role [46]. The treatment of the cryogel with the acetate buffer solution during the desorption stage produces a volume contraction in the gel (Fig. S2). In fact, the swelling degree of the cryogel decreases from 24.6 g/g to 9.1 g/g after the contact with the desorption buffer solution. This may be due to an increase in the relative abundance and stability of the carboxylic acid dimers within the polymer gel [26]. Based on physical observation, the contraction of the structure leads to a decrease in the gel's volume making intra-particle diffusion processes difficult, which also disfavor cisplatin adsorption (Fig. S2).

To improve the release of cisplatin from the cryogel and to avoid the decrease of cisplatin the adsorption on the regenerated cryogel, the desorption medium was changed to 2 mM NaOH solution (pH 9–10) (Fig. 8).

The amount of cisplatin adsorbed remains between 50 and 60 mg/g for 14 cycles and then begins to decrease gradually after the 15th cycle, accompanied by in increased desorption. As the amount of cisplatin released is expressed as a percentage of the amount adsorbed in each cycle, it is consistent that the desorbed percentage increases when the amount adsorbed decreases. It is interesting to note that despite the amount of cisplatin released during the desorption in the first cycle is only around 25%, the amount adsorbed afterwards remains fairly constant, indicating that cumulative adsorption has occurred in the cryogel. The cumulative adsorption effect can be seen in Fig. 9 where the amount of cisplatin in the cryogel increases almost lineally with the number of cycles. After 16 cycles the slope of the curve decreases, indicating that the cryogel is getting saturated with a maximum adsorption capacity of about 650 mg of cisplatin per gram of cryogel. This result is promising from the practical application point of view for the removal of the drug from pharmaceutical industries or hospital wastewater streams. In addition, it is noteworthy that the good mechanical stability of the cryogels during the adsorption/desorption studies makes it possible to regenerate the cryogel without losing its structural integrity.

4. Conclusions

In this work, poly(MAAc-co-HEMA) cryogels were synthesized by radical polymerization at sub-zero temperature. The prepared materials show good mechanical properties and high swelling degree at room temperature. The amount of cisplatin adsorbed increases with the MAAc content in the cryogel, as a result of complexation between the drug and the carboxylic group of the monomer. The cryogels demonstrated a great affinity toward cisplatin and high adsorption capacity. In addition, the possibility of reusing the synthesized material in multiple cycles for capturing the cytostatic drug in combination with the macro channels of the cryogel make this matrix a suitable candidate for the treatment of wastewater discharged from pharma industries and hospitals. The proposed technique is economical and simple to apply yet effective for the mentioned goal. Cisplatin was used as a model water pollutant in this study where the cryogel demonstrated great capability for its capture and removal. As the synthesis of cryogels has great

flexibility and the functional groups on the materials can be designed to target different types of organic compounds, use of macroporous cryogels to remove other cytostatic drug contaminants is a very promising environmental application.

Acknowledgment

The authors thank the financial support from the European Commission through the H2020-MSCA-RISE-2017 project RECOPHARMA (GA778266).

Declaration of Competing Interest

The authors declare that have no conflict of interest.

Appendix A. Supplementary material

Supplementary data to this article can be found online at https://doi.org/10.1016/j.seppur.2019.116203.

References

[1] R.A. Alderden, M.D. Hall, T.W. Hambley, The discovery and development of cisplatin, J. Chem. Educ. 83 (2006) 728–734.
[2] S. Zhu, N. Pabla, C. Tang, L. He, Z. Dong, DNA damage response in cisplatin-induced nephrotoxicity, Arch. Toxicol. 89 (2015) 2197–2205.
[3] J.P. Besse, J.F. Latour, J. Garric, Anticancer drugs in surface waters: What can we say about the occurrence and environmental significance of cytotoxic, cytostatic and endocrine therapy drugs? Environ. Int. 39 (2012) 73–86.
[4] C. Trombini, T. Garcia da Fonseca, M. Morais, T. Lopes Rocha, J. Blasco, M.J. Bebianno, Toxic effects of cisplatin cytostatic drug in mussel Mytilus galloprovincialis, Mar. Environ. Res. 119 (2016) 12–21.
[5] J. Martín, D. Camacho-Muñoz, J.L. Santos, I. Aparicio, E. Alonso, Occurrence and ecotoxicological risk assessment of 14 cytostatic drugs in wastewater, Water Air Soil Pollut. 225 (2014) 1896–1905.
[6] K. Lenz, S.N. Mahnik, N. Weissenbacher, R.M. Mader, P. Krenn, S. Hann, G. Koellensperger, M. Uhl, S. Knasmueller, F. Ferk, W. Bursch, M. Fuerhacker, Monitoring, removal and risk assessment of cytostatic drugs in hospital, Wastewater (2007) 141–149.
[7] Y. Ghafuria, M. Yunesian, R. Nabizadeh, A. Mesdaghinia, M.H. Dehghani, M. Alimohammadi, Environmental risk assessment of platinum cytotoxic drugs: a focus on toxicity characterization of hospital effluents, Int. J. Environ. Sci. Technol. 15 (2018) 1983–1990.
[8] J. Zhang, V.W.C. Chang, A. Giannis, J.-Y. Wang, Removal of cytostatic drugs from aquatic environment: A review, Sci. Total Environ. 445–446 (2013) 281–298.
[9] J. Martín, D. Camacho-Muñoz, J.L. Santos, I. Aparicio, E. Alonso, Simultaneous determination of a selected group of cytostatic drugs in water using high-performance liquid chromatography-triple-quadrupole mass spectrometry, J. Sep. Sci. 34 (2011) 3166–3177.
[10] K. Lenz, G. Koellensperger, S. Hann, N. Weissenbacher, S.N. Mahnik, M. Fuerhacker, Fate of cancerostatic platinum compounds in biological wastewater treatment of hospital effluents, Chemosphere 69 (2007) 1765–1774.
[11] P. Westerhoff, Y. Yoon, S. Snyder, E. Wert, Fate of endocrine-disruptor, pharmaceutical, and personal care product chemicals during simulated drinking water treatment processes, Environ. Sci. Technol. 39 (2005) 6649–6663.
[12] A.R. Verliefde, S.G. Heijman, E.R. Cornelissen, G. Amy, B. Van der Bruggen, J.C. van Dijk, Influence of electrostatic interactions on the rejection with NF and assessment of the removal efficiency during NF/GAC treatment of pharmaceutically active compounds in surface water, Water Res. 41 (2007) 3227–3240.
[13] N. Bolong, A.F. Ismail, M.R. Salim, T. Matsuura, A review of the effects of emerging contaminants in wastewater and options for their removal, Desalination 239 (2009) 229–246.
[14] S.A. Snyder, S. Adham, A.M. Redding, F.S. Cannon, J. DeCarolis, J. Oppenheimer, E.C. Wert, Y. Yoon, Role of membranes and activated carbon in the removal of endocrine disruptors and pharmaceuticals, Desalination 202 (2007) 156–181.
[15] W. Pronk, M. Biebow, M. Boller, Electrodialysis for recovering salts from a urine solution containing micropollutants, Environ. Sci. Technol. 40 (2006) 2414–2420.
[16] R. Broséus, S. Vincent, K. Aboulfadl, A. Daneshvar, S. Sauvé, B. Barbeau, M. Prévost, Ozone oxidation of pharmaceuticals, endocrine disruptors and pesticides during drinking water treatment, Water Res. 43 (2009) 4707–4717.
[17] A. Ghauch, A. Tuqan, H.A. Assi, Antibiotic removal from water: Elimination of amoxicillin and ampicillin by microscale and nanoscale iron particles, Environ. Pollut. 157 (2009) 1626–1635.
[18] J. Hirose, F. Kondo, T. Nakano, T. Kobayashi, N. Hiro, Y. Ando, H. Takenaka, K. Sano, Inactivation of antineoplastics in clinical wastewater by electrolysis, Chemosphere 60 (2005) 1018–1024.
[19] L.F. Delgado, S. Schetrite, C. Gonzalez, C. Albasi, Effect of cytostatic drugs on microbial behaviour in membrane bioreactor system, Bioresour. Technol. 101 (2010) 527–536.
[20] S. Hajizadeh, H. Kirsebom, A. Leistner, B. Mattiasson, Composite cryogel with immobilized concanavalin A for affinity chromatography of glycoproteins, J. Sep. Sci. 35 (2012) 2978–2985.
[21] S. Hajizadeh, B. Mattiasson, H. Kirsebom, Flow- through- mediated surface immobilization of sub-micrometre particles in monolithic cryogels, Macromol. Mater. Eng. 299 (2014) 631–638.
[22] J.W. Lim, H.F. Mohd Zaid, M.H. Isa, W.D. Oh, R. Adnan, M.J.K. Bashir, W. Kiatkittipong, D.K. Wang, Shielding immobilized biomass cryogel beads with powdered activated carbon for the simultaneous adsorption and biodegradation of 4-chlorophenol, J. Clean. Prod. 205 (2018) 828–835.
[23] E. Yeşilova, B. Osman, A. Kara, E. Tümay Özer, Molecularly imprinted particle embedded composite cryogel for selective tetracycline adsorption, Sep. Purif. Technol. 200 (2018) 155–163.
[24] S. Hajizadeh, C. Xu, H. Kirsebom, L. Ye, B. Mattiasson, Cryogelation of molecularly imprinted nanoparticles: A macroporous structure as affinity chromatography column for removal of β-blockers from complex samples, J. Chromatogr. A 1274 (2013) 6–12.
[25] S. See, P.E. Lim, J.W. Lim, C.E. Seng, R. Adnan, Evaluation of o-cresol removal using PVA-cryogel-immobilised biomass enhanced by PAC, Water SA 41 (2015) 55–60.
[26] B. Fortier-McGill, V. Toader, L. Reven, ^{1}H solid state NMR study of poly(methacrylic acid) hydrogen-bonded complexes, Macromolecules 45 (2012) 6015–6026.
[27] F.M. Plieva, J. Andersson, I.Y. Galaev, B. Mattiasson, Characterization of polyacrylamide based monolithic columns, J. Sep. Sci. 27 (2004) 828–836.
[28] E.P. Serjeant, B. Dempsey, Ionisation constants of organic acids in aqueous solution, IUPAC Chem Data Ser No. 23, New York, Pergamon, 1979, p. 74.
[29] N.A. Peppas, P. Bures, W. Leobandung, H. Ichikawa, Hydrogels in pharmaceutical formulations, Eur. J. Pharm. Biopharm. 50 (2000) 27–46.
[30] S. Yarimkaya, H. Basan, Swelling behavior of poly(2-hydroxyethyl methacrylate-co-acrylic acid-co-ammonium acrylate) hydrogels, J. Macromol. Sci. Part A Pure Appl. Chem. 44 (2007) 939–946.
[31] S. Hajizadeh, H. Kirsebom, B. Mattiasson, Characterization of macroporous carbon-cryostructured particle gel, an adsorbent for small organic molecules, Soft Matter 6 (2010) 5562.
[32] K.D. Lee, Y. Jeong, D.H. Kim, G.-T. Lim, K.-C. Choi, Cisplatin-incorporated nanoparticles of poly(acrylic acid-co-methyl methacrylate) copolymer, Int. J. Nanomed. 8 (2013) 2835–2845.
[33] B. Singh, N. Chauhan, V. Sharma, Design of molecular imprinted hydrogels for controlled release of Cisplatin: Evaluation of network density of hydrogels Ind, Eng. Chem. Res. 50 (2011) 13742–13751.
[34] X. Yan, R.A. Gemeinhart, Cisplatin delivery from poly(acrylic acid-co-methyl methacrylate) microparticles, J. Control. Release 106 (2005) 198–208.
[35] C.M. Riley, L.A. Sternson, Cisplatin, Analytical Profiles of Drug Substances vol. 14, (1985), pp. 77–105.
[36] S. Dasari, P.B. Tchounwou, Cisplatin in cancer therapy: molecular mechanisms of action, Eur. J. Pharmacol. 740 (2014) 364–378.
[37] S. Lagergren, About the theory of so-called adsorption of soluble substances, Kungliga Svenska Vetenskapsakademiens, Handlingar 24 (1898) 1–39.
[38] Y.S. Ho, Review of second-order models for adsorption systems, J. Hazard. Mater. 136 (2006) 103–111.
[39] J. Zeldowitsch, Über den mechanismus der katalytischen oxydation von CO an MnO_2, Acta Physicochem. URSS 1 (1934) 364–449.
[40] W.J. Weber, J.C. Morris, Advances in water pollution research: removal of biologically resistant pollutant from waste water by adsorption, in: Proc. Int. Conf. Water Pollution Symposium, Pergamon Press, Oxford, UK, 1962, pp. 231–266.
[41] H. Qiu, L. Lv, B.-C. Pan, Q.-J. Zhang, W.-M. Zhang, Q.-X. Zhang, Critical review in adsorption kinetic models, J. Zhejiang Univ.-Sci. A 10 (2009) 716–724.
[42] W. Rudzinski, T. Panczyk, Kinetics of isothermal adsorption on energetically heterogeneous solid surfaces: a new theoretical description based on the statistical rate theory of interfacial transport, J. Phys. Chem. 104 (2000) 9149–9162.
[43] J.A. Heimberg, K.J. Wahl, I.L. Singer, A. Erdemir, Super low friction behavior of diamond-like carbon coatings: time and speed effects, Appl. Phys. Lett. 78 (2001) 2449–2451.
[44] Y. Sağ, Y. Aktay, Kinetic studies on sorption of Cr(VI) and Cu(II) ions by chitin, chitosan and Rhizopus arrhizus, Biochem. Eng. J. 12 (2002) 143–153.
[45] C.W. Cheung, J.F. Porter, G. McKay, Sorption kinetic analysis for the removal of cadmium ions from effluents using bone char, Water Res. 35 (2001) 605–612.
[46] E. Díez-Peña, I. Quijada-Garrido, J.M. Barrales-Rienda, I. Schnell, H. Wolfgang Spiess, Advanced ^{1}H solid-state NMR spectroscopy on hydrogels, the effect of hydrogen bonding in the collapse of poly(methacrylic acid) (PMAA) hydrogels, Macromol. Chem. Phys. 205 (2004) 430–437.